32nd Annual International Conference of the IEEE EMBS
Buenos Aires, Argentina, August 31 - September 4, 2010

A Compact Dynamic Force Model for Needle-Tissue Interaction

Ali Asadian, Mehrdad R. Kermani, and Rajni V. Patel

Abstract— **In this paper, the interaction force between a surgical needle and soft tissue is studied. The force is modeled using nonlinear dynamics based on a modified LuGre model that captures all stages of needle-tissue interaction including puncture, cutting, and friction forces. An estimation algorithm for identifying the associated parameters is then presented. This approach, which is based on extended Kalman filtering (EKF), enables us to characterize the interaction with a mathematical model in the force domain. It compares the axial force measured at the needle base with its expected value and then adapts the model parameters to represent the actual interaction. To evaluate the performance of our model, experiments were performed on an artificial phantom.**

I. INTRODUCTION

Medical intervention using surgical needles is a common minimally invasive procedure. Flexible needles can be utilized for localized drug delivery, anaesthesia, radioactive seed placement or tissue biopsy especially in dealing with deep zones or regions that are difficult to access. Therefore, robotic-assisted needle insertion, which is intended to guide the needle to specific targets inside soft tissue, has become an active research area [1]. Due to several complex factors involved in the problem, accurate placement is a challenging task. These factors include (1) organ deformation; (2) target movement; (3) asymmetric needle bending as a result of tissue-needle interaction; (4) inhomogeneity, nonlinear viscoelasticity, and anisotropy of real tissue; (5) tiny anatomic structures which cannot be easily identified with common imaging modalities such as ultrasound.

On account of the fact that almost all needle steering approaches rely on a mathematical model which mimics the interaction behavior, and some of the aforementioned factors are directly linked to the force/torque signals applied to the needle by the tissue, accurate modeling is the first step toward control. Ultimately, the force model can be used either for steering purposes or in a force feedback teleoperation scheme as a surgeon assistant or as a training simulator [2]. In this regard, a force control scheme allows the slave system to insert the needle to the desired depth of penetration, and also gives the operator a realistic sense of the tissue so that the operator can take further actions.

The goal of the current work is to find a computationally feasible model that describes the relationship between the axial force measured at the needle shaft and the depth of insertion during both insertion and retraction in soft tissue. The proposed nonlinear dynamic modeling comes with an identification procedure which enables us to tune the model parameters according to tissue properties. Consequently, any change in the bio-mechanical properties of the tissue such as Young's modulus, which leads to deviation in the measured force, can be captured by the model.

This paper is organized as follows. In section II, related work in the area of tissue-needle force modeling is briefly reviewed. Section III describes the nonlinear dynamics relevant to the current work. In section IV, experimental results are given, and section V presents conclusions and suggestions for future work.

II. RELATED WORK

Okamura et al. [3] developed an empirical model for bilateral tissue-needle insertion force, which was a summation of capsule stiffness force, friction and cutting forces. According to their model, the stiffness force occurs before the puncture of the capsule while the friction and cutting forces occur right after the main puncture; however, significant variations in the liver geometry and its internal structure made a perfect match impossible. Podder et al. [4] derived a statistical model to estimate the maximum force that the needle experienced during insertion into the prostate and the perineum. Force data were collected during *in vivo* experiments to build the model based on (1) patient-specific parameters including BMI, Gleason score, prior treatments, prostate volume, and (2) procedure specific criteria such as needle size, and maximum insertion velocity.

Considering computational efficiency, most of the biophysics-based models which incorporate monitoring of elastic medium properties may not be feasible in real-time applications or be applicable to *in vivo* tests. Hing et al. [5] developed a system to predict soft tissue movement and forces under needle insertion using a linear elastic Finite Element Model (FEM) and the ABAQUS software. Two C-ARM Fluoroscopes were used to image the fiducial markers and the needle bending. Misra et al. [6] explored the sensitivity of tip axial and transversal forces to tissue rupture toughness, linear and nonlinear tissue elasticity as well as bevel angle of the needle tip. Using both contact and cohesive zone models, they incorporated these physical parameters into an FEM, and concluded that smaller bevel angles and larger tissue elasticity would result in larger tip forces.

Generally speaking, FEM is accurate for modeling small linear elastic deformations, but its computational burden is high and the accuracy is much dependent on its inputs. Misra et al. [7] summarized the rich literature in this regard. On

A. Asadian, M. R. Kermani, and R. V. Patel are with Canadian Surgical Technologies and Advanced Robotics (CSTAR) and the Department of Electrical and Computer Engineering, The University of Western Ontario, London, Ontario, Canada, aasadian@uwo.ca, mkermani@eng.uwo.ca, rajni.patel@lhsc.on.ca

R. V. Patel is also with the Department of Surgery, The University of Western Ontario, London, Ontario, Canada

the other hand, mass-spring-damper models may work fine for real-time simulations, but they have limited accuracy. Using this technique, Yan et al. [8] presented a complex on-line estimator to approximate the depth-varying tissue parameters through force measurements and a set of local polynomials. Keeping the insertion velocity constant, they validated their model using an 18Ga needle with a trihedral tip, and a two-layer phantom consisting of PVC and pork. Barbe et al. [9] proposed another on-line scheme using recursive least-squares with covariance resetting to detect abrupt transitions between tissue layers in *in vivo* conditions. Accordingly, they integrated this estimator with the Kelvin-Voigt (KV) viscoelastic interaction model to reconstruct and characterize the force evolution during insertion. Using the same interaction model, associated parallel spring and dashpot combinations were modeled by a set of piecewise linear functions in [2]. In this work, all parameters were identified with a least-squares method and based on the measurements taken at constant insertion velocity.

To the best of our knowledge, no one has ever tried to capture both insertion and retraction forces by a single model in a computationally efficient manner. The importance of finding a feasible model which can partly or fully embody required characteristics is that it paves the path to focus more on control-related issues in real-time applications.

III. A NONLINEAR FORCE MODEL FOR NEEDLE-TISSUE INTERACTION

Assuming a constant insertion velocity, the total force during the insertion and retraction phases can be dynamically modeled as a function of insertion depth using the following nonlinear state-space model. Here, z is an internal state. l and f are the depth of insertion and the axial force acting as the input and the output of our state-space model, respectively.

$$\begin{cases} \frac{dz}{dt} = l(1 - \frac{\sigma_0}{g(l)}z) \\ f = \sigma_0 zl + sign(\dot{l})l\{\sigma_1 e^{-\alpha l}(1 - \frac{\sigma_0}{g(l)}z) + \sigma_2\} \end{cases} \quad (1)$$

where,

$$g(l) = f_1 + f_2 e^{-\alpha l} \quad (2)$$

The main motivation for this selection arose from the fact that the trend describing the total insertion force as a function of insertion depth is identical to the dynamic friction provided by the LuGre model [10]. Replacing the velocity in the original the LuGre model with the insertion depth and modifying the measurement equation, the current model enables us to capture the exact force pattern. Compared to [3] and similar models, no separation is made between axial force components in this paper, and the entire procedure including both the insertion and retraction phases is described by a single set of equations. Note that the relaxation time has been ignored by this model.

As can be observed, the total force measured at the base is characterized by six parameters, namely f_1, f_2, σ_0, σ_1, σ_2, and α. Collectively, the function $g()$, which models the Stribeck effect in the original LuGre model, corresponds to the sharp drop in the insertion force once the main puncture occurs. In our model, selecting a smaller value for σ_0 leads to a bigger force peak and also a more relative force drop during the rupture. It has almost no impact on the retraction profile. Roughly speaking, changing the value of σ_1 results in the same effect on the insertion profile, but it shapes the retraction phase as well. The value of σ_2 directly affects the steady state value of the model's output, and can remove the oscillation existing in the backward motion. The role of other parameters cannot be individually interpreted. Having selected the current model, associated parameters of the proposed model are needed to be experimentally identified.

To this end, the parameters that are hardly measurable but observable can be estimated by using state-parameter estimation methods. In this paper, the estimator is realized using joint EKF (extended Kalman filter) technique. Details of the design of an EKF as a widely accepted tool in estimation theory are discussed in [11]. It is assumed here that reader is familiar with the discrete Kalman filtering. To realize the joint EKF, the original state vector (z) is augmented with new state variables (θ) which denotes the unknown coefficients of (1) [12]. The dynamics of the augmented state is assumed to be of random walk nature which is subject to zero-mean white noise perturbation (ζ). A 3rd-order Runge-Kutta algorithm is proposed to discretize the continuous model given by (1) with a proper sampling time. Let the discrete representation of the proposed dynamics at the k^{th} instant be formulated as

$$\begin{cases} z^{k+1} = F(z^k, \theta^k, l^k) + \upsilon^k \\ \theta^{k+1} = \theta^k + \zeta^k \\ f^k = H(z^k, \theta^k, l^k) + \omega^k \end{cases} \quad (3)$$

where $\theta_{6\times1}$ is the vector of model parameters as introduced beforehand; $\upsilon_{1\times1}$ and $\zeta_{6\times1}$ are the process noise while $\omega_{1\times1}$ is the measurement noise. Thus, the stochastic dynamics of the interaction force transforms into (4).

$$\begin{cases} \vartheta^{k+1} = \widetilde{F}(\vartheta^k, l^k) + \widetilde{\upsilon}^k \\ f^k = H(\vartheta^k, l^k) + \omega^k \end{cases} \quad (4)$$

where $\widetilde{\upsilon}_{7\times1}$ is the process noise of the augmented state defined by

$$\vartheta^k_{7\times1} \equiv \begin{pmatrix} z^k_{1\times1} \\ \theta^k_{6\times1} \end{pmatrix}$$

The multiple EKF is then used to estimate the augmented state vector in an asynchronous mode. In other words, the multiple approach is to alternatively run multiple filters at which a subset of the states in the $\vartheta_{7\times1}$ space is subjected to estimation and the rest of them are treated as known values [13]. Each single joint-EKF estimates a subset of the unknown parameters (θ) plus the internal state of the nonlinear dynamics (z). Once the estimation is completed at the current iteration, the model is updated with the estimated values, and then the next filter in the queue is triggered. This procedure is followed iteratively until a narrow error bound is achieved.

IV. IMPLEMENTATION AND EXPERIMENTS

A. Experimental Setup

Fig. 1 shows a general view of a compact robot which has been fully designed and manufactured in our group specifically for the purpose of prostate brachytherapy [14]. The 5-DOF manipulator can perform orientation, insertion and rotation of the needle and linear motion of the plunger to drop radioactive seeds with an average RMS targeting error of 1.45mm. A Nano43 6-DOF force/torque sensor (ATI Industrial Automation) attached to the needle holder, an Aurora electromagnetic tracker (Northern Digital Inc.) and an SSD-1000 ultrasound console (Aloka) are external sensory devices for providing feedback signals. In this test-bed, the cannula of the 18Ga stainless steel needle (Cook Medical) has a bevel angle of 22^o with outer and inner diameters of 1.270mm and 0.838mm, respectively.

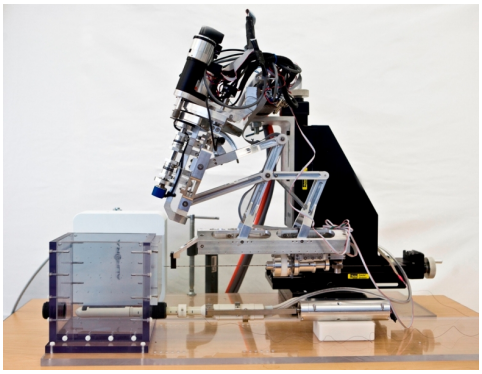

Fig. 1. A view of our brachyteraphy setup

A multi-threaded application for position/velocity control, sensor readings, and communication was developed using Microsoft® Visual C 2005, MATLAB® 2007 and the QuaRC® Toolbox (Quanser Inc.). Control computer and data capture computer were interfaced through a UDP connection over ethernet. The robot is controlled using a PID controller at the rate of 1kHz while force/torque data are acquired at the rate of 200Hz after being smoothed by a moving average filter. In order to reduce noise perturbation, a high-gain observer was implemented to estimate the velocity.

Experiments were carried out on a Gelrite Gellan Gum (Sigma-Aldrich) with a concentration rate of 4.5% in water. In order to get more consistent results, the room temperature must be controlled carefully. Keeping the gelatin in the refrigerator for a period of two weeks not only maintains the consistency, but leads to creating a thin crust on the phantom's surface which acts as a tissue membrane.

B. Experimental Results

It is presumed that the insertion trajectory is linear segment with parabolic blend (LSPB) with maximum velocity of 10mm/sec. The entire interaction was modeled under this assumption. However, exciting the system within a limited range of frequencies does not reveal all force characteristics, applying such a low-band signal is inevitable. Note that the goal of this research is to identify the unknown parameters during a regular needle insertion procedure that includes a very similar velocity profile.

As the next step, individual EKFs were tuned such that the initial error covariance matrices can be chosen to be large in order to ensure rapid convergence. Selecting the proper number of filters and pairing the states is a challenging task. Doing simulation studies and taking observability into account, three EKFs were utilized in parallel according to the definitions given in Table I. The system noise covariance matrices or $Q(\vartheta_i)$ representing the level of uncertainty in each sub-space were set as in Table I and the measurement noise variance or R was set to be 0.01 in each filter. This selection is a matter of trial and error, and the noise characteristics are assumed to be time-invariant in this paper.

TABLE I
FILTER DEFINITION

filter number (i)	state selection (ϑ_i^T)	$Q(\vartheta_i)$
$i=1$	(z, f_2, σ_0)	$0.05 \times diag(1, 10^5, 10^9)$
$i=2$	(z, f_1, σ_1)	$0.05 \times diag(1, 10^{15}, 10^{15})$
$i=3$	(z, α, σ_2)	$0.05 \times diag(1, 10^5, 10^{15})$

Inserting the needle according to the profile shown in Fig. 2 and applying the steady-state values of the estimated parameters to (1), our proposed algorithm provides an estimate of the interaction force which consists of an acceptable error bound as depicted in Fig. 3.

Note that the insertion process contributes to model the cutting force and the distributed friction whereas the retraction phase includes only friction information. Using this strategy, the interaction is characterized by the introduced set of parameters in the force domain. As a rule of thumb, provided that the sequence of estimates lies within $\pm 3\sigma$ limits, the estimation is statistically confident. To investigate this issue, a track of the standard deviations was sequentially computed until the end of the run. Fig. 4 shows the estimated values for z, σ_0, σ_2 and f_2 within the 50 millimeters of pure insertion. By comparison, estimation of σ_0 and σ_2 have the lowest confidence level and convergence rate, respectively. For the parameter α, it was noticed that in all of the conducted experiments, the estimation starts to be dominated by noise from a middle point during the insertion process. Although being observable, the contribution of α in the model's output diminishes by an increase in the value of l. This effect cannot be removed by changing the corresponding system noise parameter. Thus, to have less dependency on the noise characteristics, the value of α was assumed to be constant from the aforementioned point onward. This strategy led to more stable practical results. It is observed here that rupture is very informative for the identification procedure using EKF. Inherent lack of excitation in this system as mentioned earlier avoids a fast convergence. This problem can be partially resolved by injecting more noise into our state-space model that leads to the selected $Q(\vartheta_i)$ matrices as in Table I. As seen in Fig. 3(b) and Fig. 4, the estimation error degrades to an acceptable value and the parameters converge sufficiently after the rupture.

Finally, changing the insertion velocity to 6mm/sec and

reducing the noise covariance resulted in a more confident estimation as depicted in Fig. 5. As a critical point that has to be noticed is that the initial value of ϑ may dramatically change the performance. Achieving a better performance requires a more intricate strategy to tune the filter and is left for future work.

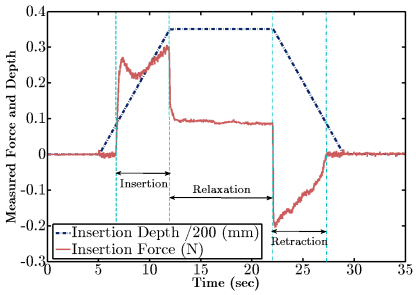

Fig. 2. Insertion profile (insertion velocity=10mm/sec)

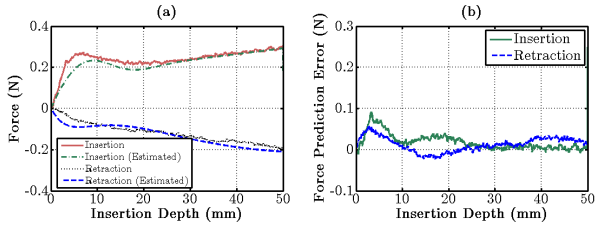

Fig. 3. (a) measurements compared with the estimations (b) force estimation error using steady-sate values of the parameters

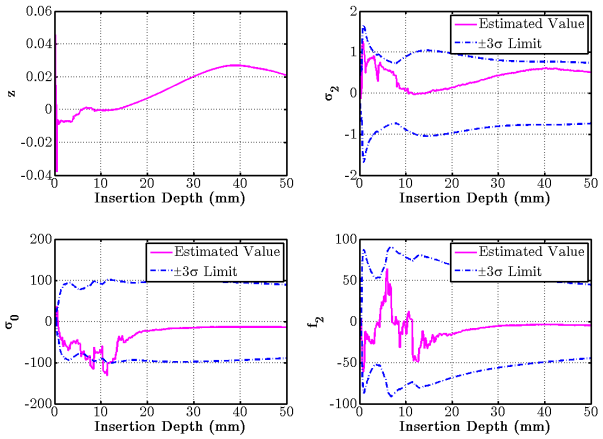

Fig. 4. State-parameter estimation (insertion velocity=10mm/sec)

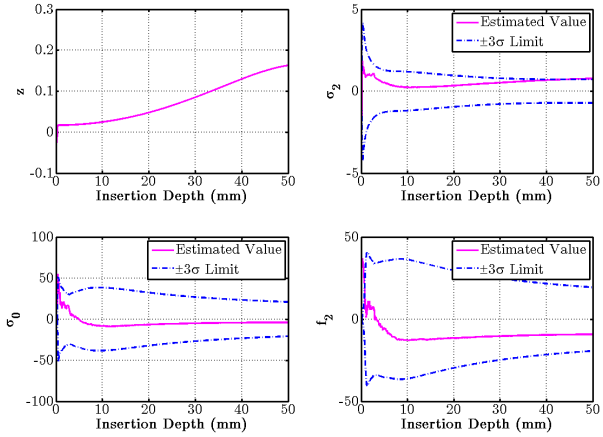

Fig. 5. State-parameter estimation (insertion velocity=6mm/sec)

V. CONCLUSION AND FUTURE WORK

In this paper, the application of asynchronous joint-EKF in needle insertion was studied. As the needle penetrates successive layers, the measurements provide a useful guide to characterize force evolution. To describe needle-tissue interaction force, a nonlinear model was first introduced and then associated parameters were adaptively identified. From the experiments, we conclude that the proposed strategy is feasible and efficient.

We plan to increase the performance of the estimator and then to extend it to a multi-layer phantom, which mimics the behavior of live tissue during percutaneous therapies. To this end, each layer consisting of a membrane plus a rigid body can be described by a set of parameters in the force domain as introduced in this paper.

VI. ACKNOWLEDGMENTS

This research was supported by the Natural Sciences and Engineering Research Council (NSERC) of Canada under grants RGPIN-1345 (R. V. Patel) and RGPIN-346166 (M. R. Kermani). The development of the robotic system for prostate brachytherapy was supported by NSERC under the Collaborative Health Research Projects Grant 262583-2003.

REFERENCES

[1] N. Abolhassani, R. Patel and M. Moallem, Needle Insertion into Soft Tissue: A Survey, *Med. Eng. Phys.*, vol. 29, 2007, pp. 413-431.

[2] P. L. Yen, R. Hibberd and B. Davies, A Telemanipulator System as an Assistant and Training Tool for Penetrating Soft Tissue, *Mechatronics*, vol. 6, no. 4, 1996, pp. 377-489.

[3] A. M. Okamura, C. Simone and M. D. O'Leary, Force Modeling for Needle Insertion into Soft Tissue, *IEEE Trans. Biomed. Eng.*, vol. 51, 2004, pp. 1707-1716.

[4] T. K. Podder, J. Sherman, E. M. Messing, D. J. Rubens, D. Fuller, J. G. Strang, R. A. Brasacchio and Y. Yu, "Needle Insertion Force Estimation Model using Procedure-specific and Patient-specific Criteria", *in 28th IEEE EMBS Annu. Int. Conf.*, 2006, pp. 555-558.

[5] J. T. Hing, A. D. Brooks and J. P. Desai, *Reality-Based Estimation of Needle and Soft-Tissue Interaction for Accurate Haptic Feedback in Prostate Brachytherapy Simulation*, Springer Tracts in Advanced Robotics, vol. 28, 2007, pp. 34-48.

[6] S. Misra, K. B. Reed, A. S. Douglas, K. T. Ramesh and A. M. Okamura, "Needle-Tissue Interaction Forces for Bevel-Tip Steerable Needles", *in 2nd Biennial IEEE/RAS-EMBS Int. Conf. on Biomedical Robotics and Biomechatronics*, 2008, pp. 224-231.

[7] S. Misra, K. T. Ramesh and A. M. Okamura, Modeling of Tool-Tissue Interactions for Computer-Based Surgical Simulation: A Literature Review, *Presence-Teleop. Virt.*, vol. 17, no. 5, 2008, pp. 463-491.

[8] K. G. Yan , T. Podder, D. Xiao, Y. Yu, T. Liu, C. Cheng and W. S. Ng, An improved needle steering model with online parameter estimator, *Int. J. Comput. Assist. Radiol. Surg.*, vol. 1, no. 4, 2006, pp. 205-212.

[9] L. Barbe, B. Bayle, M. de Mathelin and A. Gangi, In Vivo Model Estimation and Haptic Characterization of Needle Insertions, *Int. J. Rob. Res.*, vol. 26, no. 1112, 2007, pp. 1283-1301.

[10] M. R. Kermani, R. V. Patel and M. Moallem, Friction Identification and Compensation in Robotic Manipulators, *IEEE Trans. Instrum. Meas.*, vol. 56, no. 6, 2006, pp. 2346-2353.

[11] C. K. Chui and G. Chen, *Kalman Filtering with Real-Time Applications*, Edition 4, Springer Berlin Heidelberg; 2008.

[12] P. Moireau, D. Chapelle and P. L. Tallec, Joint State and Parameter Estimation for Distributed Mechanical Systems, *Comput. Methods Appl. Mech. Engrg.*, no. 197, 2008, pp. 659-677.

[13] L.P. Yan, B. S. Liua, and D. H. Zhou, The Modeling and Estimation of Asynchronous Multirate Multisensor Dynamic Systems, *Aerosp. Sci. Technol.*, no. 10, 2006, pp. 63-71.

[14] H. S. Bassan, R. V. Patel and M. Moallem, A Novel Manipulator for Percutaneous Needle Insertion: Design and Experimentation, *IEEE/ASME Trans. Mechatron.*, vol. 14, no. 6, 2009, pp. 746-761.